

Influence of Grain Size on the Band-gap of Annealed SnS Thin Films

Priyal Jain^a and P. Arun^{b*}

^aDepartment of Electronic Science,
University of Delhi, South Campus
Delhi 110021

^bMaterial Science Research Lab,
S.G.T.B. Khalsa College,
University of Delhi, Delhi - 110 007, India

July 13, 2012

Abstract

The manuscript reports the variation in optical band-gap of vacuum annealed SnS thin films. The samples were characterized by using X-Ray Diffraction, UV-visible Spectroscopy and Raman Analysis. Results show that while annealing does not effect the polycrystalline sample's lattice structure or unit cell size it does control the grain size. The band-gap (E_g) increases with increase in grain size. E_g values were found to be very high (1.8-2.5 eV) for samples studied.

Keywords Thin Films, Chalcogenides, UV-visible spectroscopy

*email:arunp92@physics.du.ac.in, Telephone:091 011 29258401, Fax: 091 011 27666220

1 Introduction

Tin sulphide (SnS) is a semiconducting material formed from elements belonging to the IV-VI group of the periodic table. Research on SnS shows that it has potential use as holographic or optical data storage medium [1, 2]. Also, due to its high absorption coefficient (of the order $\sim 10^4 \text{ cm}^{-1}$) and bandgap $\sim 1.3 - 1.6 \text{ eV}$, SnS films have been used as photovoltaic devices [3, 4]. SnS exists in various crystallized states like orthorhombic [5], tetrahedral (Zinc blende like) [6] or a highly distorted rock-salt (NaCl) structure [7]. Due to the nature of the tin and sulphur bondings, it forms two dimensional sheets [8], giving rise to a layered structure with strong intra-planar forces and weak Van der Waal forces between the adjacent planes [9, 10]. Films of SnS have been fabricated using various techniques such as thermal evaporation [11], RF sputtering [12], chemical vapour deposition [13], electrodeposition [14], spray pyrolysis [15] and sulphurisation of metallic precursors [16]. The optical properties of SnS strongly depend on the deposition method used [17]-[21]. While a maximum band gap (1.78 eV) was reported in films obtained by wet chemical method [5], the lowest band-gap (1.12 eV) was reported for films made by chemical bath deposition [17].

The deposition techniques influences the film's grain size, crystal structure and residual strain which in turn effect the optical properties of the film. In light of the increasing importance of SnS and its potential applications, it becomes important to study the film structure with its band-gap. Thus, in this manuscript we report our studies on vacuum evaporated SnS thin films that were vacuum annealed after fabrication and try to establish a relation between their structural and optical properties.

2 Experimental

SnS films of varying thicknesses were fabricated by thermally evaporating powdered SnS at vacuum better than $\sim 4 \times 10^{-5}$ Torr in a Hind High Vac (12A4D) thermal evaporation coating unit. The depositions were made on glass microscopy slides maintained at room temperature. SnS powder of 99% purity supplied by Himedia(Mumbai) was used as the starting material. The thickness of the asgrown films were measured by a Veeco Dektak Surface Profiler (150). The samples were then subjected to post-annealing temperatures under vacuum for 30 mins at 373 K and 473 K. The structural, morphological and optical characterisations were done systematically for both the as grown and annealed films. We report and compare here the structural, morphological and optical properties of annealed samples of five different thicknesses, 270, 480, 600, 650 and 900 nm. The stuctural analysis were done using Bruker D8 Diffractometer. The Raman spectra of the films were obtained with Renishaw Invia Raman Microscope using Argon laser beam in the reflection mode. The surface morphology of the samples were examined with FEG-SEM JSM7600F. The optical properties of the samples were carried out using Systronics UV-VIS Double beam Spectrophotometer (2202).

3 Results and Discussion

The Raman spectra were collected from back scattered Ar^{2+} laser. Analysis of all our samples were done maintaining constant beam area, exposure time (30 sec) and power (30 mW). All the samples without exception showed three peaks, two prominent peaks around 170 cm^{-1} and 238 cm^{-1} . The 330 cm^{-1} peak is associated with SnS_2 [22]. The ~ 170 and 238 cm^{-1} Raman peaks are associated with those of single crystal SnS [5]. Our peak positions are slightly displaced from these positions. Figure (1) shows representative Raman spectra of a 900nm thick film, before annealing (rt) and after annealing at 373 K and 473 K respectively. The relative contribution of the 330 cm^{-1} peak in annealed samples is lower as compared to that in as grown samples. Annealing, hence, removes SnS_2 bonding/ defects formed during film fabrication. The 170 cm^{-1} or the B_{2g} mode's peak corresponds to interaction along the inter-layer 'b' axis, while the 238 cm^{-1} peak is the A_g mode that corresponds to the symmetric Sn-S bonding stretching mode in the a-c plane [23]. It is clear from figure (1) that the relative contributions from B_{2g} and A_g do not change on annealing.

Figure (2) exhibits the X-Ray diffractograms of thin annealed (473 K) SnS films of different thicknesses. Three prominent peaks are seen at $2\theta \sim 31^\circ$, 37° and 43° . These peak positions matched with those reported in ASTM Card No. 83-1758. The SnS in our samples hence exists with orthorhombic unit cell structure with the (040) peak having the maximum intensity. While there are many works in the literature that show (040) peak to be the most intense [24, 25], others have reported (111) peak to be the most intense [5, 26]. This again underlines how growth technique and conditions influence the character of the SnS films. The Miller indices of the remaining prominent peaks are also indicated in figure. The lattice parameters ‘a’, ‘b’ and ‘c’ of SnS in single crystal state are given as 4.148, 11.48 and 4.177 Å, respectively.

We have evaluated the lattice parameters ‘b’ from the (040) peak’s position, followed by which we calculated ‘a’ and ‘c’ from the (200) and (131) peak positions. The lattice parameters of the annealed samples at 5.76, 11.36 and 4.01 Å were found to be different from those of SnS in single crystal state. While the variation in ‘b’ and ‘c’ maybe be considered marginal, there is a significant change in ‘a’. Albanesi et al [10] have done systematic analyses to understand the effect of changing unit cell size on SnS band-gap. Their study suggest an increase in volume of the unit cell would lead to a lowering in SnS band-gap. We shall return to this when we discuss the results of our optical studies. While there is a significant change in the lattice constants (namely ‘a’) as compared to that of single crystal, we find that they do not change with film thickness or annealing temperature. Figure (3A) shows all three lattice parameters remaining unaffected with film thickness. Since points coincides, each point in this graph represents samples annealed at 373 K and 473 K. The difference in lattice constant present (a_{obs}) with respect to that given in the ASTM (a_{ASTM}) implies that the grains are in a state of stress with the peaks shifting left compared to those reported in the ASTM, we conclude tensile residual stresses are acting within the grains [27]. However, a_{obs} is constant for all the samples hence the same tensile residual stress exists in all the samples. This tensile residual stress thus appears as a background in our study. While the lattice parameters remain unaltered, the grain size changes with annealing. The grain size reported were calculated using the Full Width at Half Maxima (FWHM) of the diffraction peaks in Scherrer’s formula [28]. From figure (3B), it is clear that there is a persistent increase in grain size with annealing, however this effect is more pronounced in thinner films. The grain size increases from 120 nm to 250 nm in the 270 nm films while this increase in grain size with annealing temperature is impeded for thicker films (fig 3B).

SnS are layered compounds with zig-zagged molecules of SnS forming layers. These layers stack one on top of the other along the ‘b’ axis with weak Van der Waal ‘inter-planar’ forces acting between the layers. The layers themselves because of the zig-zagging have finite thickness and along the ‘b’ axis have strong ‘intra-planar’ forces acting within it. Ehm [29] has shown that application of pressure decreases inter-planar distances along ‘b’ axis without disturbing intra-planar spacing. As stated above, the Raman B_{2g} peak represents vibrations along the ‘b’ axis. It would appear thinner films with larger grain size have vibrations taking place at lower wave-number than thicker films with smaller grains.

Fig (4) shows the variation of Raman peak position of annealed samples. While the A_g peak remains fixed at 226.5 cm^{-1} , the B_{2g} peak shows a systematic shift to a higher wavenumber with increasing film thickness. In our case, a thicker annealed film also implies smaller grain size. The Raman peak’s position and its FWHM is a rich source of information. While it does give information on the structure, the corroborative X-ray diffraction study showing no variation in lattice parameters imply variation in Raman spectra is indicative of something else. Literature on Raman Analysis have shown variation of FWHM to be a measure of phonon confinement [30, 31] with shift in peak position related to grain size [31]-[35] and nature of defect on the grain boundaries [30]. A shift to higher wavenumbers is indicative of smaller grain size. Hence, the results of X-Ray diffraction and Raman Analysis put together suggest that annealed SnS thin films have large grains with grain size decreasing as the annealed film thickness increases. This is best understood from fig (5).

The results shown in figure (3B) are also reflected in the Scanning Electron Microscope’s micrographs. The thinner film 480 nm annealed shows significant increase in grain size and grain density when annealed at higher temperature as compared to the 900 nm thick film. Comparing the 900 nm thick films annealed at 373 K and 473 K respectively, we do not find such improvement in grain size or density as inferred from the X-Ray diffraction analysis. Based on the structural and morphological results, it would be interesting to study the

optical properties of these samples. Since the lattice parameters and residual tensile stress on the grain's bulk remains same with only grain size and to an extent grain density varying in the samples, the study should reveal the contribution grain size has on the properties like band gap, E_g .

The optical absorption and transmittance spectra of all the samples were obtained in wavelength range 300-900 nm. The absorption spectras were typical with absorption increasing near band-edge. Tin sulphide is known to have both direct band-gap [36] and indirect band-gap [5]. The band-gap can be evaluated using the absorption coefficient (α) obtained from the UV-visible spectra. The band-gap is obtained using the relation [37]

$$\alpha h\nu = (h\nu - E_g)^n$$

where 'n=1/2' for direct allowed transitions. On plotting a curve between $(\alpha h\nu)^2$ with respect to $h\nu$, on fitting a line on the linear part of the curve, the point where it cuts the 'X-axis' gives the energy band-gap of the sample. Using this method, we have evaluated band-gaps for all the samples. As discussed earlier, the lattice parameters remained unchanged for annealed films, hence the bandgap variation is not caused by the lattice defects.

The bandgap of SnS films strongly depends on the deposition process and the film parameters like the film thickness. SnS amorphous film of thickness 1000 nm grown on a glass substrate by spray pyrolysis has a bandgap of 1 eV [15]. While film grown by vacuum evaporation were found to be polycrystalline with bandgap varying between 1.15-1.3 eV. The variation in bandgap was found to be related to the distance between the source and the substrate [26]. Films grown on ITO substrates by pulsed electrodeposition were polycrystalline in nature with bandgap being 1.34 eV [24]. Polycrystalline films grown by chemical bath deposition on glass substrates of 290 nm thickness also possess low bandgap (1.15 eV) [17]. While the films grown with RF sputtering technique are also polycrystalline, they have very high bandgaps varying from 1.3 to 1.7 eV [12]. A recent study [38] on SnS polycrystalline thin films grown by thermal evaporation reports SnS band-gap between 2.15-2.28 eV. Clearly, polycrystalline SnS films have higher band-gaps compared to their amorphous counterparts.

Figure (7) shows the grain size dependence of the bandgap. The bandgap increases with the increasing grain size. Table 1 summarizes the findings of this study. It shows on annealing thinner films have larger grains. The large grain size gives the annealed samples an enhanced band-gap. Thicker films however, have smaller grains and lower band-gap. The bandgap of a sample is broadly affected by its chemical composition, crystal structure, grain size and defects. Of all these contributing parameters, except for grain size, all other parameters remain constant. While the larger volume of the unit cell leads to an initial low E_g (~ 1.8 eV) as explained by Albanesi [10], grain size contribute to an increase in E_g of vacuum annealed SnS samples.

Conclusion

Thin films of SnS were fabricated by thermal evaporation on microscopy glass slides at room temperature. These films when annealed in vacuum at 373 K and 473 K developed a tensile strain along the lattice 'ac' plane. The magnitude of this tensile strain was independant of the film thickness and annealing temperature. However, the film thickness and annealing temperature play an important influencing role on the samples grain size. We conclude from our results that E_g of polycrystalline SnS films strongly depends on grain size.

Acknowledgment

Authors are thankful to the Department of Science and Technology for funding this work under research project SR/NM/NS-28/2010. We are also grateful to Dr Chhaya Ravi Kant, Department of Applied Sciences, IGIT (GGS-IP University, Delhi) for extending lab facilities.

References

- [1] M. Radot, Rev. Phys. Appl., **18**, (1977) 345 .
- [2] S.G. Patil and R.H. Tredgold, J. Pure Appl. Phys., **4**, (1971) 718.
- [3] Zhijie Wang, Shengchun Qu, Xiangbo Zeng, Junpeng Liu, Changsh Zhang, Furui Tan Lan Jin and Zhanguo Wang, Journal of Alloys and Compounds, **482** (2009) 203.
- [4] H. Noguchi, A. Setiyadi, H. Tanamora, T. Nagatomo and O. Omato, Sol. Energy Mater. Sol. Cells, **35** (1994) 325.
- [5] S. Sohila, M. Rajalakshmi, Chanchal Ghosh, A.K. Arora and C. Muthamizhchelvan, Journal of Alloys and Compounds, **509** (2011) 5843.
- [6] C. Gao, H. Shen, T. Wu, L. Zhang and F. Jiang, Mater. Lett., **64** (2010) 2177.
- [7] A.N. Mariano and K.L. Chopra, Appl. Phys. Lett., **10** (1967) 282
- [8] T. Jiang and G A Ozin, J. Mater. Chem., **8** (1998) 1099.
- [9] P.M. Nikolic, P. Lj Miljkovic, B. Mihajlovic and B. Lavrencic, J. Phys. C: Solid Status Phys., **10** (1977) L289.
- [10] L. Makinistian and E.A. Albanesi, Comput. Mater. Sci., **50** (2011) 2872.
- [11] M.M.E.I. Nahass, N.M. Zeyada, M.S. Aziz and N.A.E.I. Ghamaz, Opt. Mater., **20** (2002) 159.
- [12] Katy Hartman, J.L. Johnson, Mariana I. Bertoni, Daniel Recht, Micheal J. Aziz, Micheal A. Scarpulla and Tonio Buonassis, Thin Solid Films, **519** (2011) 7421.
- [13] M.T.S. Nair and P.K. Nair, Semicond. Sci. Technol., **6** (1991) 132.
- [14] A. Ghazali, Z. Zainal, M.Z. Hussein and A. Kassim, Sol. Energy Mater. Sol. Cells, **55** (1998) 237.
- [15] B. Thangaraju and P. Kaliannan, J. Phys. D: Appl. Phys., **33** (2000) 1054.
- [16] K.T. Ramakrishna Reddy and P. Purandhara Reddy, Mater. Lett., **56** (2002) 108.
- [17] Chao Gao, Honglie Shen and Lei Sun, Appl. Surf. Sci., **257** (2011) 6750.
- [18] K.T. Ramakrishna Reddy, P. Purandhara Reddy, P.K. Datta and R.W. Miles, Opt. Mater., **17** (2001) 295.
- [19] G.H. Yue, D.L. Peng, P.X. Yan, L.S. Wang, W. Wang and X.H. Luo, Journal of Alloys and Compounds, **468** (2009) 254.
- [20] M Devika, N Koteeswara Reddy, K Ramesh, K R Gunasekhar, E S R Gopal and K T Ramakrishna Reddy, Semicond. Sci. Technol., **21** (2006) 1125.
- [21] A. Ortiz, J.C. Alonso, M. Garcia and J. Toriz, Semicond. Sci. Technol., **11** (1996) 243.
- [22] G. Lucovsky, J. C. Mikkelsen, W. Y. Liang, R. M. White and R. M. Martin, Phys. Rev. B, **14** (1976) 1664.
- [23] H.R. Chandrasekhar, R.G. Humphreys, U. Zwick and M. Cardona, Phys. Rev. B, **15**, (1977) 2177.

- [24] G.H. Yue, W. Wang and L.S. Wang, Journal of Alloys and Compounds, **474** (2009) 445.
- [25] Feng Jiang, Honglie Shen, Chao Gao, Bing Liu, Long Lin and Zhou Shen, Appl. Surf. Sci., **257** (2011) 4901.
- [26] M. Devika, N. Koteeswara Reddy, D. Sreekantha Reddy, S. Venkatramana Reddy, K Ramesh, E S R Gopal, K R Gunasekhar, V Ganesan and Y B Hahn, J. Phys.: Condens. Mater., **19** (2007) 1.
- [27] A.L. Patterson, Phys. Rev., **56** (1956) 978.
- [28] B.D. Cullity and S.R. Stock, "Elements of X-Ray Diffraction", 3rd Ed., Prentice-Hall Inc (NJ, 2001).
- [29] L. Ehm, K. Knorr, P. Dera, A. Krimmel, P. Bouvier and M. Mezouar, J. Phys.:Condens. Mater., **16** (2004) 3545.
- [30] Kuninori Kitahara, Toshitomo Ishii, Junki Suzuki, Takuro Bessyo and Naoki Watanabe, INT J. Spectrosc., **2011** (2011) 1.
- [31] Hyun Chul Choi, Young Mee Jung and Seung Bin Kim, J. Of Vib. Spectrosc., **37** (2005) 33.
- [32] Rajalakshmi M, Arora A.K., Bendre B.S., Mahamuni S, J. Appl. Phys., (2000) **87** 2445.
- [33] Yang C.L., Wang J.N., Ge W.K., Guo L., Yang S.H., Shen D.Z., J. Appl. Phys., (2001) **90** 4489.
- [34] Guo L, Yang S, Yang C, Yu P, Wang J, Ge W, Wong G.K.L., Appl. Phys. Lett., (2000) **76** 2901.
- [35] Alim K.A., Fonoberrov V.A., Baladdin A.A., Appl. Phys. Lett., (2005) **86** 053103.
- [36] M. Devika, N. Koteeswara Reddy, M. Prashantha, K. Ramesh, S. Venkatramana Reddy, Y.B. Hahn and K.R. Gunasekhar, Phys. Status Solidi A, 207, No. **8**, (2010) 1864.
- [37] K. Kamano, R. Nakata and M. Sumita J Phys. D: Applied Physics, **22** (1989) 136.
- [38] Shuying Cheng and Gavin Conibeer, Thin Solid Films, **520** (2011) 837.

Figures Captions

1. A representative Raman spectra of a 900 nm thick SnS film before and after annealing at temperatures indicated.
2. X-Ray Diffraction patterns of SnS films of thicknesses (a) 270, (b) 480, (c) 600, (d) 630 and (e) 900 nm after annealing at 373 K.
3. Graphs show the variation of (a) lattice constants with film thickness (annealed films) and (b) Grain size with annealing temperature. These results were obtained from the X-Ray Diffraction Patterns.
4. The variation in Raman A_g and B_{2g} peak positions of annealed (373 K and 473 K) SnS films with film thickness.
5. The B_{2g} peak position of Raman spectra varies with grain size. The graph shows shift of Raman peak to lower energy level with increasing grain size.
6. SEM micrographs show grain size improvement in thinner film (480 nm) when annealed at higher temperature. However, the 900 nm films show no variation in grain size on annealing.
7. The band-gap of annealed SnS films were found to be linearly proportional to the grain size.

4 Tables

Table 1: *A comparison of state in which a very thin and thick SnS films exists in.*

	Thin film	Thicker film
Grain Size	Large	Small
E_g	Large	Lower

Figures

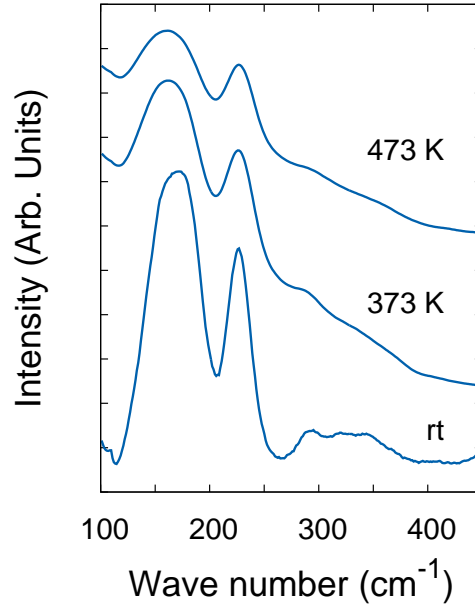


Figure 1: *A representative Raman spectra of a 900 nm thick SnS film before and after annealing at temperatures indicated.*

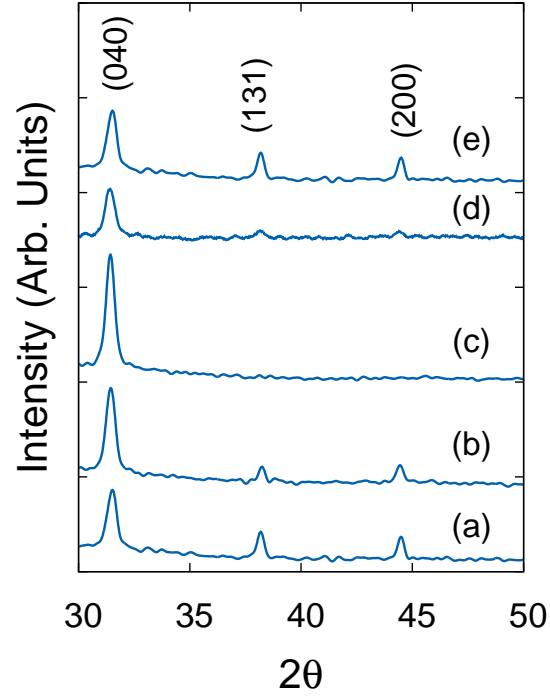


Figure 2: X-Ray Diffraction patterns of SnS films of thicknesses (a) 270, (b) 480, (c) 600, (d) 630 and (e) 900 nm after annealing at 373 K.

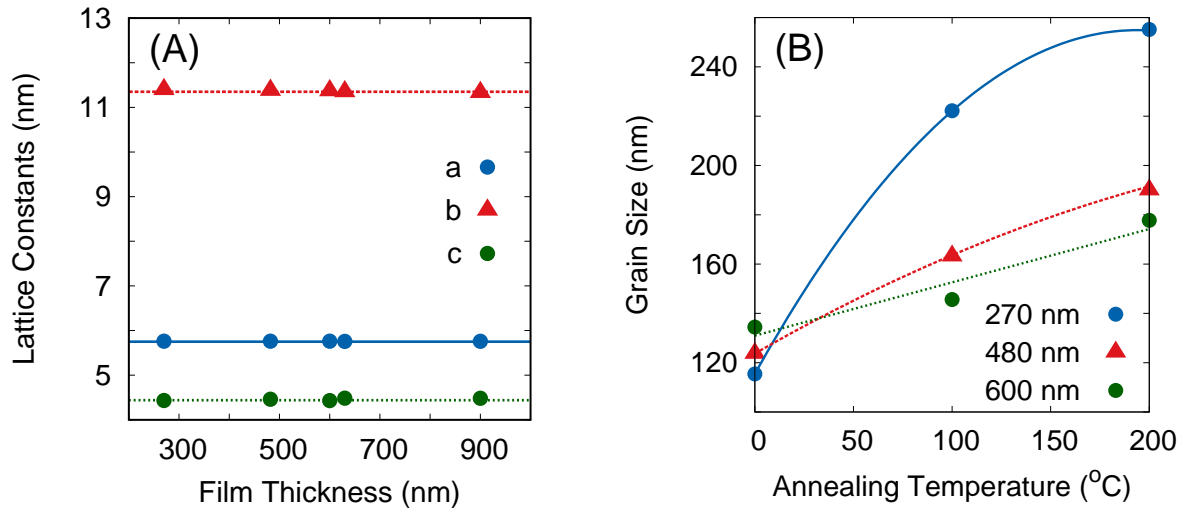


Figure 3: Graphs show the variation of (A) lattice constants with film thickness (annealed films) and (B) Grain size with annealing temperature. These results were obtained from the X-Ray Diffraction Patterns.

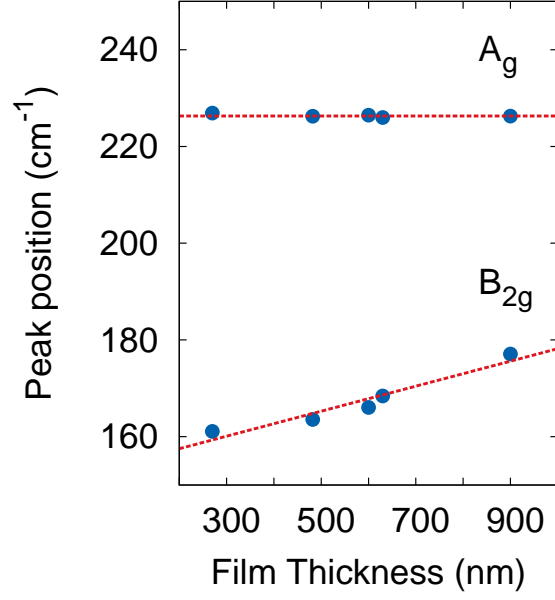


Figure 4: The variation in Raman A_g and B_{2g} peak positions of annealed (373 K and 473 K) SnS films with film thickness.

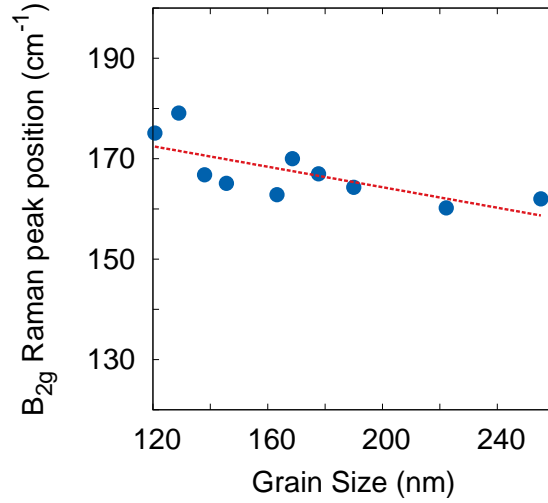


Figure 5: The B_{2g} peak position of Raman spectra varies with grain size. The graph shows shift of Raman peak to lower energy level with increasing grain size.

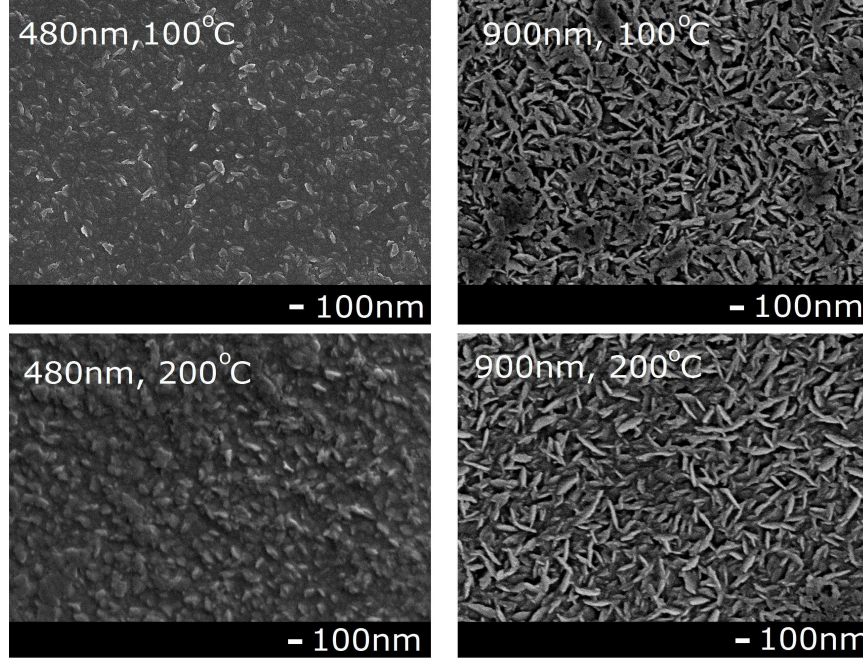


Figure 6: SEM micrographs show grain size improvement in thinner film (480 nm) when annealed at higher temperature. However, the 900 nm films show no variation in grain size on annealing.

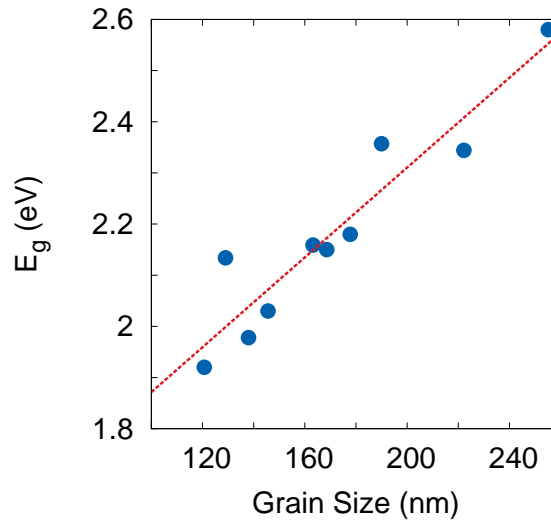


Figure 7: The band-gap of annealed SnS films were found to be linearly proportional to the grain size.